

## Time-Dependent Hartree-Fock-Bogoliubov Calculations of Heavy-Element Fusion and Fission Phenomena

R. Y. Cusson<sup>(a)</sup> and H. W. Meldner

Lawrence Livermore Laboratory, Livermore, California 94550

(Received 28 August 1978)

Time-dependent Hartree-Fock-Bogoliubov calculations in three dimensions are reported for the fusion of two  $^{118}\text{Pd}$  isotopes and subsequent fission of the compound nucleus  $^{236}\text{U}$ . Constant-strength pairing, and simplified Skyrme plus Yukawa and Coulomb interactions were included. A new result is the appearance of (nonaxial) surface oscillations in the compound or fissioning systems.

The TDHF (time-dependent Hartree-Fock) approximation uses just a two-body interaction to produce detailed descriptions of heavy-ion scattering and fusion/fission phenomena. Its computational complexity has been tackled successfully in calculations of  $^{236}\text{U}$  fission dynamics<sup>1</sup> for the  $l=0$  axial case, as well as the determination of fusion cross sections,<sup>2</sup> deflection functions,<sup>3</sup> and other features<sup>4-6</sup> that can be compared with experiments. Perhaps the most elaborate three-dimensional (3D) calculation<sup>4</sup> to date was performed for  $^{20}\text{Ne}(164\text{ MeV}) + ^{56}\text{Ni}$  with constant fractional occupation of the orbits, while the most extended 2D work involved the constant-gap approximation for the fission of  $^{236}\text{U}$  (Ref. 1).

This note describes a 3D calculation with the constant-strength dynamical pairing model of Belyaev<sup>7</sup> for the fission of  $^{236}\text{U}$  after fusion in the symmetric system  $^{118}\text{Pd} + ^{118}\text{Pd}$  (at a Pd laboratory energy of 5.4 MeV/nucleon). The colliding ions are enclosed in a box of dimensions  $27.6 \times 27.6 \times 16\text{ fm}^3$ , and a coordinate grid spacing of 1.2 fm in all three directions suffices to ensure conservation of total energy and of free-motion kinetic energy to 1% or better during a collision. The system is constrained to be symmetric about the scattering plane (the  $YZ$  plane).

The initial wave function for the  $^{118}\text{Pd}$  fragments

is obtained by performing static Hartree-Fock-Bogoliubov (HFB) iterations.<sup>8</sup> Each orbit is assumed to contain four nucleons with an effective charge of  $0.39e$ , and the direct part of the Coulomb potential is computed exactly with the help of the fast-Fourier-transform algorithm and the boundary Green's function. The interaction used is the simplified Skyrme plus Yukawa developed earlier for TDHF use.<sup>9</sup> The strength of the pairing interaction is adjusted during the static HFB iterations to produce a gap parameter  $\Delta = 1.03\text{ MeV}$ . Thirty-four orbits including  $M$  multiplicities are included in the HFB basis. They are  $(n, l) = (0, 0), (0, 1), (0, 2), (1, 0), (0, 3), (1, 1), (0, 4),$  and  $(1, 2)$ . With the present interaction and choice of  $\Delta$ , the Fermi energy is at  $-8.94\text{ MeV}$  so that the  $(0, 4)$  orbit with a single-particle energy of  $-11.5\text{ MeV}$  is almost fully occupied ( $\nu^2 = 0.965$ ) and the  $(1, 2)$  orbit at  $-9.0\text{ MeV}$  is only partially occupied ( $\nu^2 = 0.16$ ).

Table I and Figs. 1-3 give some of our results for the various impact parameters considered. Three impact-parameter regions are of particular interest. The peripheral region results in small energy losses ( $\leq 1\%$ ) and scattering angles within a few degrees of the grazing angle. In this region the fragment elongation variable  $\sigma$  of Möller and Nix<sup>10</sup> changes by just a few percent and no

TABLE I. Collisions of  $^{118}\text{Pd}(E_{\text{lab}} = 637\text{ MeV}) + ^{118}\text{Pd}$ , at various impact parameters.

Impact parameter $b$ (fm)	Center-of-mass deflection angle $\theta$ (deg)	Coulomb deflection angle (deg)	Final c.m. kinetic energy (MeV)
8.8	$57 \pm 1$	57	$318.5 \pm 1$
8.5	$59 \pm 1$	58.7	$317.5 \pm 1$
8.0	$60 \pm 1$	61.7	$310 \pm 1$
7.0	$37 \pm 1$	68.7	$215 \pm 10$
3.0	Fused	116	Fused
2.0	Fused	135	Fused

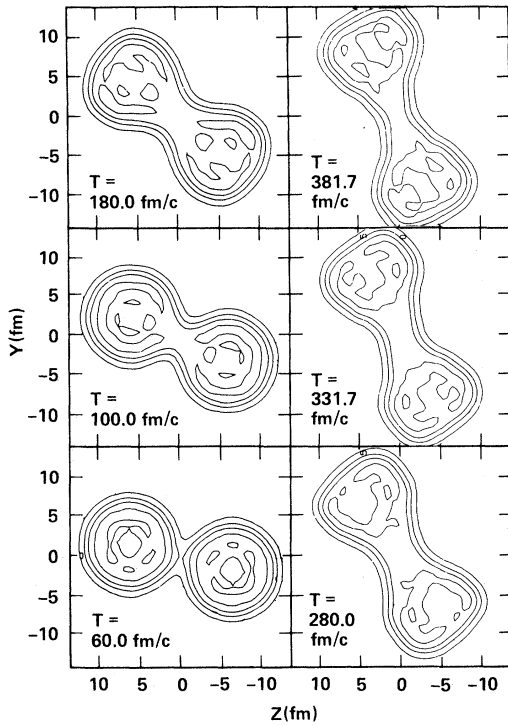


FIG. 1.  $^{118}\text{Pd}(E_{\text{lab}} = 637 \text{ MeV}) + ^{118}\text{Pd}$  at impact parameter  $b = 7.0 \text{ fm}$ . The incoming total angular momentum is  $L = 210\hbar$  while the outgoing orbital one is  $165\hbar$ . These pictures illustrate a fusion-fission event. At  $T = 60 \text{ fm/c}$  the fragments separation is  $13.3 \text{ fm}$ ,  $\sigma = 2.705$ , and the relative motion kinetic energy is  $88 \text{ MeV}$ . The transition from the fusion to the fission valley begins at this time and is manifested by a rapid rise in  $\sigma$ . At  $T = 100 \text{ fm/c}$  the system is at the distance of closest approach  $r = 13.1 \text{ fm}$ ; here  $\sigma = 2.78$  and is rising. The snapshot at  $T = 180 \text{ fm/c}$  shows the maximum neck size attained in this collision; by now  $r = 13.6$ , and  $\sigma = 2.89$ .  $T = 280 \text{ fm/c}$  refers to maximum  $\sigma = 3.06$ ; here  $r = 15.05$  and  $L_{\text{orb}} = 165\hbar$ . There are no further decreases in  $L_{\text{orb}}$  after this time. The fifth picture has  $r = 15.9$ ,  $\sigma = 3.04$ , and the last frame shown has  $r = 16.8$ ,  $\sigma = 3.07$ . The integration was stopped at this time because of the edge effect. An extrapolation to scission yields a scission time of  $440 \pm 20 \text{ fm/c}$  at which time  $r = 18.2 \pm 0.5 \text{ fm}$ .

substantial neck formation occurs during the collision; i.e., the fragments do not deform noticeably. The second region is characterized by a large increase ( $\approx 10\%$ ) in  $\sigma$  before separation, i.e., by a transition from the fusion to the fission valley. The sequences of pictures shown in Fig. 1 illustrate this effect at an impact parameter  $b = 7.0 \text{ fm}$ . This second region occupies most of the impact-parameter range. For  $b \lesssim 3 \text{ fm}$  we have fusion; the third region of interest. The value  $b = 3 \text{ fm}$  corresponds to a fusion cross sec-

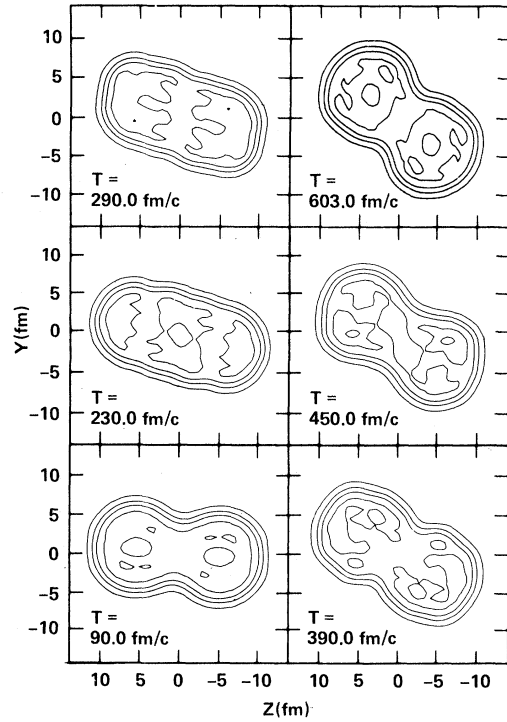


FIG. 2.  $^{118}\text{Pd}(E_{\text{lab}} = 637 \text{ MeV}) + ^{118}\text{Pd}$  at impact parameter  $b = 2.0 \text{ fm}$ ,  $L_{\text{in}} = 60\hbar$ , illustrating a fusion event. The minimum separation  $r = 9.6 \text{ fm}$  is reached at  $T = 150 \text{ fm/c}$ . The separation remains at this value until  $T = 300 \text{ fm/c}$ . Between  $T = 300$  and  $480 \text{ fm/c}$  the separation increases to  $10.7 \text{ fm}$  and begins to decrease again. The relative-motion kinetic energy at all times after fusion remains under  $7 \text{ MeV}$ , less than half of which is radial kinetic energy. The fragment elongation parameter  $\sigma$  remains at  $2.7 \pm 0.025$  until  $T = 140 \text{ fm/c}$ . It then increases to an average value of  $2.8$ .

tion of  $280 \text{ mb}$ . This is somewhat higher than the values obtained by Nix and Sierk in a recent classical hydrodynamics study.<sup>11</sup> The reason for the different result in TDHFB seems to be that the present calculation includes (effective single particle) viscosity which decreases the compound-system total angular momentum during the collision. This in turn leads to a lowering of the centrifugal barrier and therefore favors fusion. The small-impact-parameter sequence is illustrated in Fig. 2. These snapshots can only illustrate a small fraction of the observed dynamics. The corresponding movie films have been obtained and show clearly the presence of surface waves and oscillations in all cases except the peripheral ones. The case studied here results in a total c.m. excitation energy of only about  $80 \text{ MeV}$ . This is less than  $0.35 \text{ MeV/nucleon}$  in the c.m.

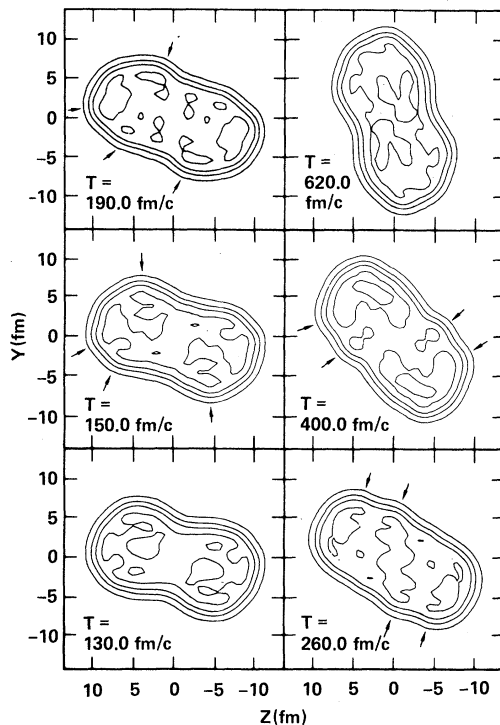


FIG. 3.  $^{118}\text{Pd}(E_{\text{lab}} = 637 \text{ MeV}) + ^{118}\text{Pd}$  at impact parameter  $b = 3.0 \text{ fm}$ ,  $L_{\text{in}} = 90\%$ . These snapshots illustrate the nonaxial surface collective modes. The first picture, at  $T = 130 \text{ fm/c}$ , shows a smooth surface with a characteristic overall nonaxiality. At  $T = 150 \text{ fm/c}$  several bumps have appeared, some of which are indicated by arrows. These effects appear independent of the grid size used. The distance from bump to bump is about  $5 \text{ fm}$ . The deviation from a smooth surface is of order  $0.5\text{--}0.7 \text{ fm}$ .

system. Yet much of the surface dynamics is unmistakably nonaxial in nature as is indicated by Fig. 3. The typical wavelength is about  $5 \text{ fm}$ ; the amplitude is about  $0.6 \text{ fm}$  and the propagation velocity of these waves is near  $0.07c$ . Because of their nonaxial nature these surface waves do not appear in 2D calculations<sup>3</sup> constrained to axial symmetry. These waves also travel in the direction perpendicular to the scattering plane. The conclusion appears to be that neither the 2D approximation nor the separable approximation can adequately describe the complexity of heavy-system dynamics. The present results also show variations in the value of  $\Delta$ , the gap parameter, during the nonperipheral scattering. The gap decreased by as much as 50% when a large fraction

of the collective energy was transformed into internal energy.

These results demonstrate the feasibility of TDHFB calculations for heavy ions and show the existence of surface waves, a fusion-fission transition, and a complete-fusion impact-parameter region. This approximation provides some nonclassical insight into the time scales and "modes" of fusion-fission dynamics. Further work should include the separation of neutrons and protons and a spin-orbit term for the calculation of effects from neutron excess and shell structure.

We acknowledge stimulating discussions with W. M. Howard. This work was performed under the auspices of the U. S. Department of Energy by the Lawrence Livermore Laboratory under Contract No. W-7405-ENG-48.

(a)Permanent address: Physics Department, Duke University, Durham, North Carolina 20706.

<sup>1</sup>J. W. Negele, S. E. Koonin, P. Möller, J. R. Nix, and A. J. Sierk, *Phys. Rev. C* **17**, 1098 (1978).

<sup>2</sup>H. Flocard, S. E. Koonin, and M. S. Weiss, *Phys. Rev. C* **17**, 1682 (1978); P. Bonche, B. Grammaticos, and S. Koonin, *Phys. Rev. C* **17**, 1700 (1978).

<sup>3</sup>K. T. R. Davies, V. Maruhn-Rezwani, S. E. Koonin, and J. W. Negele, Oak Ridge National Laboratory Report, July, 1978 (unpublished).

<sup>4</sup>R. Y. Cusson, J. A. Maruhn, and H. W. Meldner, *Phys. Rev. C* **18**, 2589 (1978).

<sup>5</sup>R. Y. Cusson, G. Gomez-del Campo, J. A. Maruhn, and V. Maruhn-Rezwani, to be published.

<sup>6</sup>R. Y. Cusson, G. Gomez-del Campo, and H. W. Meldner, Lawrence Livermore Laboratory Report No. UCRL-81179 (unpublished); in Proceedings of the Third International Conference on Clustering, University of Manitoba, June 19-23, 1978 (to be published).

<sup>7</sup>S. T. Belyaev, *Nucl. Phys.* **64**, 17 (1965); see also J. Blocki and H. Flocard, *Nucl. Phys.* **A273**, 45 (1976).

<sup>8</sup>The fast-Fourier-transform method and a sixth-order predictor-corrector algorithm are used [see Ref. 4 and 6, and R. Y. Cusson, R. K. Smith, and J. A. Maruhn, *Phys. Rev. Lett.* **36**, 1166 (1976)], to propagate the solution in time. The computing method utilizes fully optimized array-processing routines (STACKLIB) developed for Control Data Corp. computers at Lawrence Livermore Laboratory.

<sup>9</sup>P. Bonche, S. Koonin, and J. W. Negele, *Phys. Rev. C* **13**, 1226 (1976).

<sup>10</sup>P. Möller and J. R. Nix, *Nucl. Phys.* **A272**, 5026 (1976).

<sup>11</sup>J. R. Nix and A. J. Sierk, *Phys. Rev. C* **15**, 2072 (1977).